

Candidate drug molecule-DNA interaction and molecular modelling of candidate drug molecule

 Ayça Karasakal¹,  Yelda Yalçın Gürkan²,  Sülünay Parlar³

¹Tekirdağ Namık Kemal University, Faculty of Science and Letters, Department of Chemistry, Tekirdağ, Turkey

²Tekirdağ Namık Kemal University, Faculty of Science and Letters, Department of Chemistry, Tekirdağ, Turkey

³Ege University, Faculty of Pharmacy, Department of Pharmaceutical Chemistry, İzmir, Turkey

Cite this article as: Karasakal A, Yalçın Gürkan Y, Parlar S. Candidate drug molecule-DNA interaction and molecular modelling of candidate drug molecule. J Health Sci Med 2022; 5(6): 1547-1555.

ABSTRACT

Aim: 1,4-dihydropyridine derivative, 1-(3-phenyl propyl)-4-(2-(2-hydroxybenzylidene) hydrazone)-1,4-dihydropyridine (abbreviated as DHP) was synthesized as potential agent for Alzheimer's disease which is a progressive neurodegenerative brain disorder affecting millions of elderly people. With this study, the electrochemical properties of DHP were investigated and its interaction with DNA was analyzed by differential pulse voltammetry (DPV) and cyclic voltammetry (CV) measurements. In addition, this study aims to determine degradation mechanism of the DHP molecule by Density-functional theory (DFT) in gas and in aqueous phase.

Material and Method: Experimental conditions such as immobilization time, the effect of the scan rate, concentration, and the effect of pH were optimized. The method was validated according to validation parameters such as range, precision, linearity, limit of detection (LOD), limit of quantitation (LOQ) and inter/intraday.

Results: Linearity study for the calibration curve of DNA and DHP with DPV was calculated in the calibration range 10-100 µg/mL. The LOD and LOQ values were calculated as 3 and 10 µg/mL and intra-day and inter-day repeatability (RSD %) were 1.85 and 3.64 µg/mL, respectively. After the DHP-DNA interaction, the oxidation currents of guanine decreased as a proof of interaction. The activation energy of the most possible path of reaction was calculated, and their thermodynamically most stable state was determined in gas phase.

Conclusion: We developed to improve a sensitive, fast and easy detection process for determination of interaction between DHP and DNA.

Keywords: DNA, candidate drug molecule, DNA-drug interaction, biosensor, DFT

INTRODUCTION

Electrochemical biosensors have an important impact on environmental monitoring, clinical diagnosis and pharmaceutical studies. From the electrochemical studies, useful information can be attained with regard to redox process (1). DNA biosensors offer fast, basic, and high sensitivity and they are inexpensive in the determination of drug-DNA interaction. They consist of a nucleic acid recognition layer immobilized to the electrochemical transducer. The nucleic acid recognition layer detects changes in DNA structure or the specific sequence of DNA that occurs during the interaction of DNA and binding molecules (2-5). The interaction of drugs with DNA is one of the main targets in drug discovery. The search for a drug-DNA interaction has a significant effect on understanding the mechanism of interaction

in order to design more efficient drugs. Drug and DNA interaction studies associated with ligands that bind DNA such as intercalation, cross linking, non-covalent binding and covalent binding do exist in literature. The different molecular interaction types such as electrostatic, van der Waals, hydrogen bonding, dipole-dipole and π - π interactions cause different pharmacological effects (6-8). The specificity, speed, portability and low-cost usage of biosensors enable them to be utilized in many areas from clinical applications to pharmaceutical research, from food analysis to agricultural analysis. It can be observed that the analysis results are more specific and sensitive for the detection of hereditary diseases and contagious infections (9). The results of the analysis of substance-DNA interaction are obtained by monitoring the changes

in the signals of the substance itself or the electrophilic bases in the DNA structure. Wang et al. (10) investigated daunomycin and DNA interaction in solution phase by using carbon paste electrode, and Dogan-Topal et al. (11) analyzed Leuprolide and DNA interaction and guanine signals decreased after the interaction with leuprolide in their study.

In this study, DNA interactions of the synthesized compound DHP were analyzed with the help of electrochemical methods. DHP was previously synthesized as a potential compound for Alzheimer's disease (AD) (12). Alzheimer's disease is one of the leading causes of death among elderly people in the world (13). Existing drugs have been unable to combat or reverse the progression of the disease. This is due to the complex and multifactorial nature of AD. A great deal of research has been devoted to the development of new anti-AD agents. There are many studies based on the treatment of AD with different heterocyclic scaffolds (14). Efforts have also been made towards the development of pyridine scaffolds as anti-AD agents (15). One of the most popular methods for the preparation of pyridines is the oxidation of corresponding 1,4-dihydropyridines. 1,4-dihydropyridine is viewed as a privileged scaffold as a brain-targeting chemical delivery system (CDS) which is based on the dihydropyridine-pyridinium type redox conversion of a lipophilic dihydropyridin (16). Due to the therapeutic role of the pyridine (17-20) derivatives and the pharmaceutical effects of 1,4-dihydropyridine compounds (12,21,22), in this study we intend to explore the effects of a 1,4-dihydropyridine derivative. **Figure 1** shows molecular structure of DHP. We aim to develop novel electrochemical DNA biosensor for DHP and DNA interaction. The goal of the study is to determine a predicted degradation pathway for DHP molecular structure in gas and aqueous phase. Most possible reaction pathway for DHP molecular structure to occur with OH radicals was determined by employing density functional theory (DFT) method.

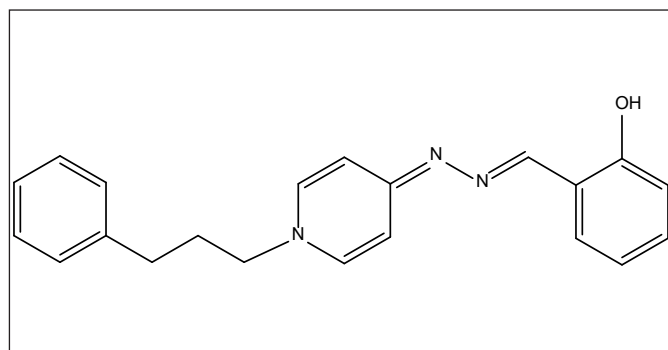


Figure 1. Molecular structure of DHP.

MATERIAL AND METHOD

The ethics committee approval isn't required in the article.

Chemistry

Apparatus and instruments: The IR spectra of the compound was monitored by attenuated total reflectance (ATR) (PerkinElmer Spectrum 100 FT-IR, Shelton, USA). ^1H NMR spectra was recorded with a Varian AS 400 Mercury Plus NMR spectrometer (Varian, Palo Alto, CA, U.S.A.) operated at 400 MHz. in deuterio-DMSO. Abbreviations for data quoted are: s (singlet), t (triplet), quin (quintet), m (multiplet), dd (doublet-doublet). Mass spectra (ESI-MS) was measured on a Thermo MSQ Plus LC/MS (Thermoscientific Inc., San Jose, CA). All chemicals used for synthesis were purchased from Sigma, Acros, Fluka, and Merck companies.

Synthesis of the compound DHP: The synthesis of the final compound DHP was prepared in three steps in our previous study (12). In the first step, a solution of 4-chloropyridine (0.1 mol) and hydrazine monohydrate (0.2 mol) in 1-propanol (30 mL) was refluxed for 18h. The solution was cooled to 0°C and the precipitate was filtered, washed with cool 1-propanol and crystallized from ethanol. In the second step, 4-hydrazinylpyridine (7.5 mmol) was condensed with 2-hydroxybenzaldehyde in ethanol (30 mL) to obtain hydrazone intermediate. The precipitate was filtered and washed with cool ethanol/water (1:1) mixture and crystallized from ethanol. In the third step, a mixture of hydrazone intermediate (0.01 mol) and 3-phenylpropyl bromide (0.02 mol) were refluxed in ethanol. The mixture was cooled to room temperature. The precipitate was filtered and washed with cool ethanol. The crude product was crystallized from ethanol. Then, it was converted to its' 1,4-dihydropyridine form after being treated with sodium hydroxide solution.

Spectral data of compound DHP: IR (KBr) cm^{-1} : 3025, 2925, 2856, 1646, 1598, 1513, 1454, 1400, 754, 700. ^1H NMR (400 MHz, DMSO- d_6) δ ppm: 8.39 (1H, s, N=CH), 7.47 (1H, dd, $J = 2.0, 7.8$ Hz, Ar-H), 7.39-7.33 (2H, m, Pyr-H), 7.29-7.15 (6H, m, Ar-H), 6.87-6.84 (2H, m, Ar-H), 6.50 (1H, dd, $J = 2.7, 7.4$ Hz, Pyr-H), 6.21 (1H, dd, $J = 2.7, 7.4$ Hz, Pyr-H), 3.78 (2H, t, $J = 7.2$ Hz, N- CH_2 - CH_2 - CH_2 -Ph), 2.55 (2H, t, $J = 8.0$ Hz, N- CH_2 - CH_2 - CH_2 -Ph), 1.97 (2H, quin, $J = 7.4$ Hz, -N- CH_2 - CH_2 - CH_2 -Ph). ESI-MS m/z : 332 (M+H).

DNA and Candidate Drug Molecule

Reagents and chemicals: Double stranded deoxyribonucleic acid (dsDNA) obtained from fish sperm and KH_2PO_4 , K_2HPO_4 , $\text{K}_3(\text{Fe}(\text{CN})_6)$, $\text{K}_4(\text{Fe}(\text{CN})_6)$, CH_3COOH , NaCl, NaOH were supplied from Sigma-Aldrich.

Apparatus and instruments: AUTOLAB-PGSTAT 30 electrochemical analysis system was studied in voltammetric measurements. A pencil graphite electrode (PGE) (Tombow 0.5 HB) was used as the working electrode, a Ag/AgCl electrode was employed as the reference electrode, and a platinum wire was used as the counter electrode. μ -AUTOLAB with NOVA software was used in DPV and CV measurements.

Preparation of Solutions

Preparation of DHP: Alptuzun et al. (12) synthesized the final molecule. The chemical name of the molecule is 1-(3-phenyl propyl)-4-(2-(2-hydroxybenzylidene)hydrazono)-1,4-dihydropyridine (abbreviated as DHP). Figure 1 shows the chemical structure of DHP. 1 mg DHP was dissolved in DMSO (dimethyl sulfoxide). Stock solutions of DHP were diluted with BBS. Each pretreated electrode was immersed into the vials containing DHP solution (40 μ g/mL) during 5-90 min. Immobilized electrodes were rinsed with BBS.

Preparation of DNA: Double stranded DNA (ds-DNA) (abbreviated as DNA) from fish sperm was used. 1 mg DNA was prepared in purified water. Stock solutions of DNA was diluted with PBS. Activated electrodes were immersed in 200 μ g/mL of DNA solution for 5-60 min. and DNA immobilized electrodes were rinsed with PBS.

Preparation of buffer solutions: 0.5 M acetate (pH 4.8), 0.05 M phosphate (pH 7.4) and 0.10 M borate buffer solutions (pH 8.1) were prepared by diluting with 20 mM NaCl.

Method

Electrode Activation: The PGEs surface were activated by application of +1.40 V for 30 s in ACB in order to oxidize -COOH groups of the PGEs. Passive adsorption was used for the immobilization of DHP and DNA.

Interaction of DNA with DHP: Firstly, PGEs were immobilized with DNA. DNA coated electrodes were immersed into the vials containing 40 μ g/mL DHP solution prepared in BBS for during 5-45 min. DHP and DNA immobilized electrodes were rinsed with PBS and BBS, respectively.

Measurement

ACB was used in all DPV measurements. The oxidation signals were measured by scanning from +0.3 V to +1.2 V potential range vs. Ag/AgCl/3 M reference electrode. 20-100 mV/s were used for the scan rate measurements. 10 mM $K_3(Fe(CN)_6)/K_4(Fe(CN)_6)$ solution was used for CV measurements.

Methodology and Computational Set-up

Computational models: The molecules were modelled by using distances of mean bonds and the geometrical

parameters corresponding to the benzene ring. For the computational modeling; (i) the sp^3 -hybridized carbon that formed tetrahedral angles was employed and (ii) the sp^2 -hybridized C-O atoms that composed 120° angles were employed. The planar aromatic ring kept unchanged, excluding the position of attack. It was presumed that the C-H bond was creating a tetrahedral angle with the attacking $\bullet OH$. This phenomenon is explained in the literature as the hybridization state change of the carbon atoms from sp^2 to sp^3 at the addition center (23).

In photocatalytic degradation reactions of DHP, some products that are more harmful than that original material contains could be formed. The reactions of photocatalytic degradation for DHP along with its hydroxy derivatives were directly correlated with the reaction of $\bullet OH$ with these molecules, since the production yield was the same. Therefore, the analysis of theoretical reaction kinetics of DHP was conducted only for $\bullet OH$. The study started with the initiation of DHP and then continued with the exposure of $\bullet OH$ in order to complete the reaction. The reaction yields were modelled and calculated in gas phase. Experimental results found in literature showed that the detachment of a hydrogen atom from saturated hydrocarbons by $\bullet OH$ was realized first, and then unsaturated hydrocarbons along with the materials with similar structure received the previously mentioned $\bullet OH$ (24). For this purpose, the determination of possible reaction pathways was studied thoroughly for the analyzed reactions. Density functional theory (DFT) was utilized for the electronical orbital calculations of the reactant molecule, yield, and transition state complexes, which were realized for each reaction path, along with their optimized geometries. In order to conduct the conformational analysis of the structures, a potential energy surface (PES) scan using the B3LYP/6-31G* method was performed in a relaxed manner, which meant optimization criteria was reached for each point, along with the torsional coordinates for both conformers (25).

Methodology: Optimized geometry of the reactants, the products, and the transition state complexes were calculated with DFT method via the Gaussian 09 software (26). DFT methods utilize the precise electron density in order to compute properties of the molecular structure and electronic energy levels, which includes electron correlation, as well. For open-shell systems, spin contamination is not an issue of concern, therefore this type of calculation becomes favourable. The combination of the Hartree-Fock and Becke exchange terms along with the Lee-Yang-Parr correlation functional which created the hybrid B3LYP functional were a good fit for the DFT calculations that were conducted in this study (23).

The determination of the basis set for the calculations is of utmost importance. The study employed a popular and well-studied B3LYP/6-31G(d) level. For the transition state determination, the reaction coordinates were defined as the forming C–O bonds in the addition paths. As in abstraction paths, the forming of H–O bond was defined. The structures for ground state and transition state were approved by conducting a frequency analysis study at the previously mentioned level. The characterization of the transition structures was established by detecting one imaginary frequency. This frequency corresponded to a first-order saddle point, belonging to the reaction coordinate. The B3LYP/6-31G(d) level was also used for the calculations of zero-point vibrational energies (ZPEs) (23).

RESULTS

Optimization Conditions of DNA

Optimum conditions for DNA immobilization are given in **Figure 2**. DNA was prepared in pH 4.8 ACB, pH 7.4 PBS (20 mM NaCl) and 7.4 PBS (500 mM NaCl) buffer solutions. The effect of buffer solution is presented in **Figure 2A**. The highest oxidation currents of guanine were found in PBS (20 mM NaCl), so DNA solutions were prepared in PBS (20 mM NaCl). To determine the optimum concentration of DNA, DNA solutions were prepared in PBS so that they could be in the range of 5–100 µg/mL (**Figure 2B**). Oxidation currents of guanine ascended together with increasing DNA concentration and then leveled off. 100 µg/mL of DNA was used for optimum DNA concentration because the highest peak current was observed. For optimization of the immobilization time, DNA was immobilized during 5- 60 min (**Figure 2C**)

The oxidation currents of guanine increased for 30 min and then started to decrease so 30 min was chosen for an optimum immobilization time.

Optimization Conditions of DHP

Optimization conditions of DHP were investigated. DHP has an irreversible anodic peak potential at +0.8 V. Figure 3A and 3B show experimental results such as immobilization time and concentration. pH 4.8 (ACB),

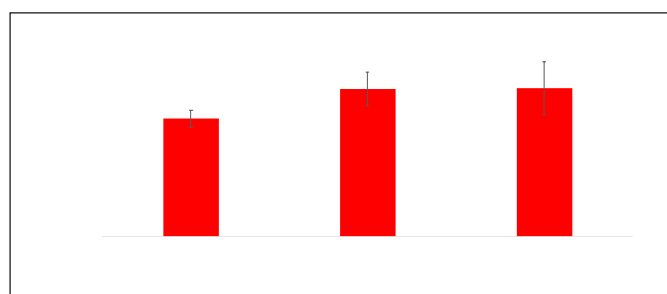


Figure 2A. Average current of guanine oxidation signals measured with DNA for different pH (n:5)

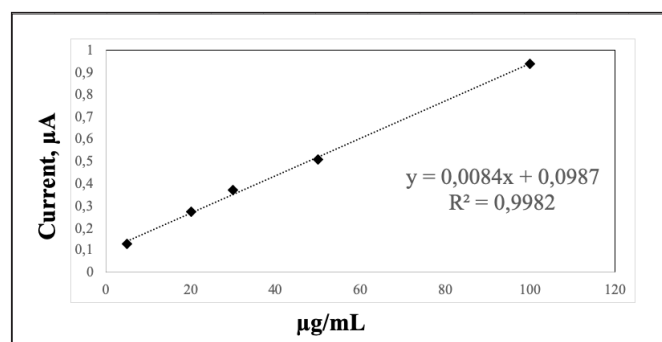


Figure 2B. Average current of guanine oxidation signals measured with DNA for different concentration. (n:5)

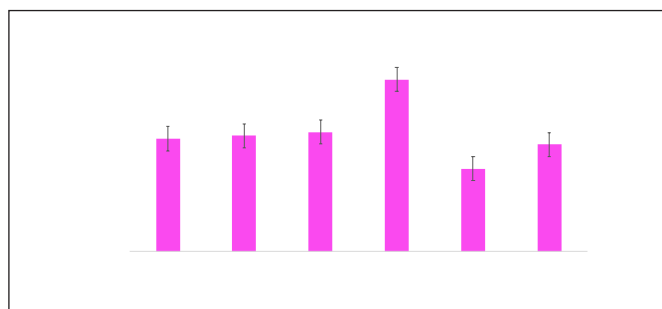


Figure 2C. Average current of guanine oxidation signals measured with DNA for different immobilization time (n:5).

pH 7.4 (PBS) and pH 8.1 (BBS) buffer solutions were analyzed for optimum pH. The highest DHP oxidation signals were obtained in BBS. In order to find the optimum concentration of DHP, DHP solutions were prepared in BBS so that the final concentrations could be in the range of 10–100 µg/mL. (**Figure 3A**). The maximum signal was detected at 100 µg/mL but 40 µg/mL DHP was used in the experiments because reproducible and sufficient signal was obtained in 40 µg/mL. The effect of immobilization time is given in **Figure 3B**.

To determine optimum immobilization time of DHP, DHP was immobilized during 10-90 min. The oxidation signals of DHP increased with the time and remained stable after 45 min. 45 min was used for optimum immobilization time. The calibration curves ($y=mx+n$) were constructed by the plots of the peak current (y) of DHP versus the concentrations (x) of the calibration standards. Linearity was observed in the range 10-100 µg/mL.

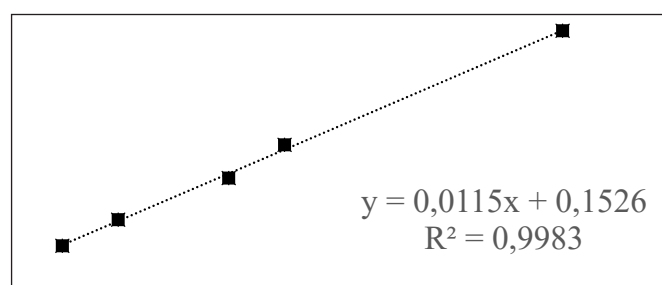


Figure 3A. DHP current corresponding to the oxidation signal for different concentration. (n:5)

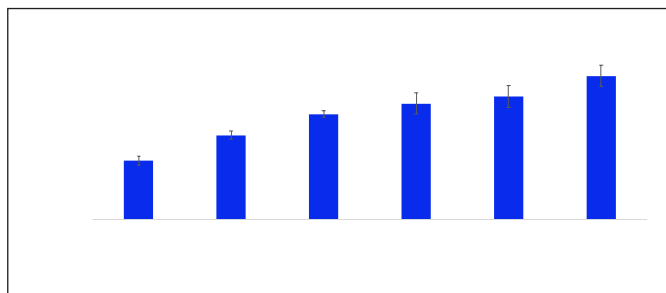


Figure 3B. DHP current corresponding to the oxidation signal for different immobilization time. (n:5)

The regression equation: $y=0.0115x+0.1526$ ($R^2:0.9983$)

where y is the peak current, and x is the concentration of DHP in $\mu\text{g/mL}$. LOD and LOQ were calculated to be $3.3 \sigma/m$ and $10 \sigma/m$, respectively, where m is the slope of the calibration curve and σ is the standard deviation of the intercept of the regression equation (27). Values of LOD and LOQ were calculated to be 3 and $10 \mu\text{g/mL}$, respectively. Different three concentrations were measured in three replicates during the same day and three consecutive days to determine the precision and accuracy of developed method. The precision of the method was given as the relative standard deviation (RSD %). The intra- and inter-day precision values were found to be 1.85 and $3.64 \mu\text{g/mL}$.

Effect of Scan Rate

Scan rate studies were carried out with CV. It was investigated whether it was diffusion or adsorption controlled in order to determine the effect of the scan rate. The results for the effect of the scan rate are given in **Figure 4**.

As it is seen from **Figure 4**, the peak currents of DHP increased with increasing scan rate (10 to 100 mV/s).

The equations peak current versus scan rate for $40 \mu\text{g/mL}$ DHP prepared in BBS are as follow:

$I_{p1} (\mu\text{A})=0.0668(\text{mVs}^{-1})+0.3912$ ($R^2=0.9967$) for the first peak

$I_{p2} (\mu\text{A})=-0.007(\text{mVs}^{-1}) - 0.25$ ($R^2=1.00$) for the second peak

The slope of the above equations are close to the theoretical value of 0.5, which proved the occurrence of a diffusion-controlled electrode process for the first and second peak according to these results (30).

The electrochemical reaction was found as diffusion controlled. The equations peak current versus the root of scan rate are as follow:

$I_{p1} (\mu\text{A})=0.8883v^{1/2}(\text{mVs}^{-1})^{1/2} - 2.0878$ ($R^2=0.9864$)

$I_{p2} (\mu\text{A})=-0,1016v^{1/2}(\text{mVs}^{-1})^{1/2}+0.0832$ ($R^2=0.9882$)

Effect of pH

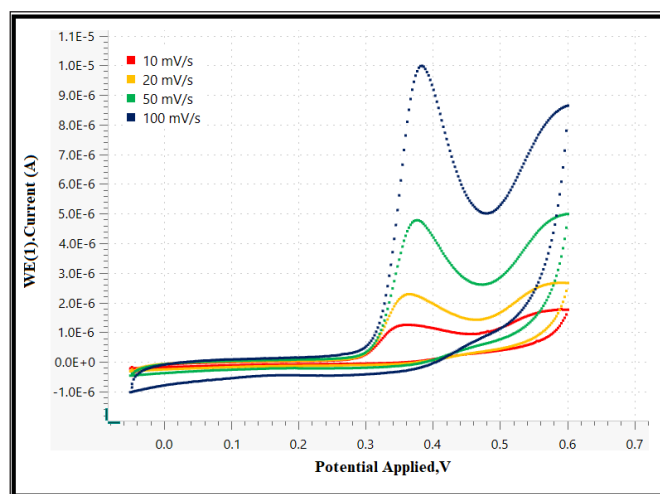


Figure 4. Cyclic voltammograms of DHP at different scan rates (10–100 mV/s). (n:5)

The effect of pH was investigated with CV. DHP oxidation signal values obtained at different pH 's are given in **Figure 5**. DHP was prepared and measured in ACB (4.8), PBS (7.4) and BBS (8.1). The order of the pH was determined to be $\text{PBS} > \text{BBS} > \text{ACB}$. The peak potential values were observed from $+0.35 \text{ V}$ to $+0.6 \text{ V}$.

Interaction

DNA and DHP interaction was investigated to explain the effect of DHP on DNA. DHP and DNA were interacted in different interaction times (5–45 min) by DPV (**Figure 6**). After the interaction with DHP, guanine oxidation signals decreased. 15 min was selected as the optimum interaction time.

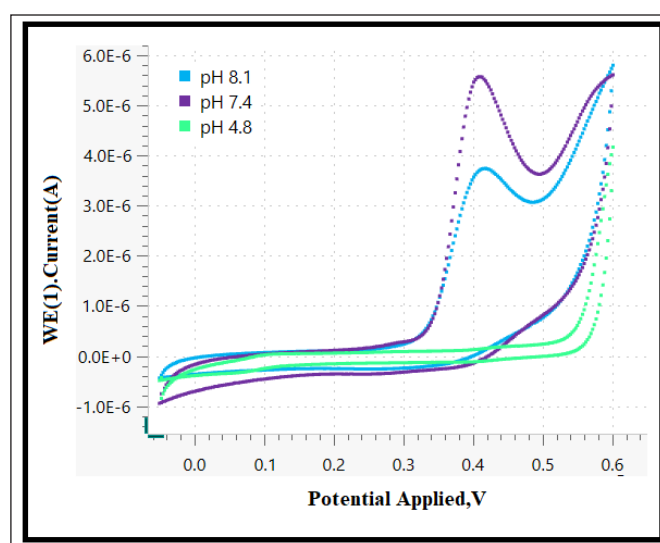


Figure 5. Cyclic voltammograms of DHP at different pH.

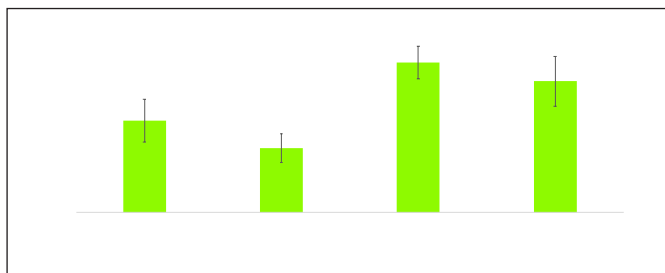


Figure 6. Histogram of oxidation currents of DNA and DHP interaction. (n:5)

Molecular Modeling

DFT reactivity descriptors were used in order to have a deeper understanding of the most susceptible radical attack sites for hydroxyl, which in turn enlightens the photocatalytic degradation reaction of DHP. The molecular geometry of DHP molecule and the numbering system, which is optimized with previously mentioned method and level that is used along the calculations (Figure 7).

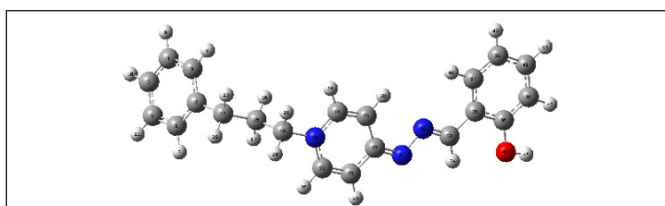


Figure 7. Optimized structure of DHP and the numbering system (gray, carbon; red, oxygen; blue, nitrogen; white, hydrogen).

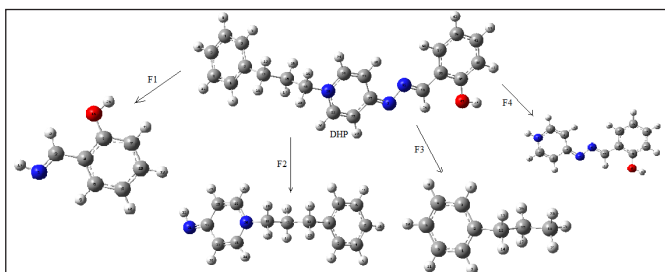


Figure 8. Possible pathways for the photocatalytic degradation of DHP.

Three most probable reaction paths are shown in Figure 8. The close softness values to the $\bullet\text{OH}$ radical of these paths were the selection criteria. It is well-known that the most stable structure geometry corresponds to the lowest-energy structure of the molecule. Constant energy, Enthalpy and Gibbs free energy values visualized by DFT are given Table 1.

Table 1. Constant energy, Enthalpy and Gibbs free energy values according to DFT Method			
Molecules	Energy (kcal/mol)	Enthalpy (kcal/mol)	Gibbs free energy (kcal/mol)
DHP	-660082.807	-660082.215	-660131.909
F1	-251490.149	-251489.557	-251515.028
F2	-409335.277	-409372.334	-409372.134
F3	-219627.906	-219627.314	-219654.847
F4	-441197.817	-441197.225	-441232.324

DISCUSSION

Voltammetric signals of dsDNA electroactive bases were used for interactions between drug and DNA and DNA and drug interactions, which explain changes in the electrochemical responses of DNA before and after the interaction with drugs. As a simple method of base immobilization for working electrodes, physical adsorption is widely utilized. This method also eliminates the requirement for modifications and chemical reagents. In our study, physical (passive) adsorption was used for DNA immobilization on pencil graphite electrodes (28-30) As a rule of thumb, the researches of electrochemical based DNA-drug interaction, which are mostly label free, depend on the alterations in variations in the oxidation indicators of guanine bases due to the fact that guanines are the most electroactive bases within thymine, cytosine and adenine. Guanines have high levels of oxidation capacity at +1.0 V (versus reference electrode) whereas sugar and phosphate backbone, which generate other parts of nucleic acids, are non-electroactive. Utilizing guanine bases as in electrochemical studies provides an opportunity as pencil graphite, carbon and gold electrodes adsorb them without any difficulty (28). If DHP and DNA are not immobilized on the surface of PGEs, the guanine signals cannot be obtained and repeated.

100 $\mu\text{g}/\text{mL}$ of DNA concentration was utilized since it led to the most steady signals with the highest intensity. Immobilization time is shown to be one of the most important experimental parameters in effective DNA immobilization onto the surface of the electrode. The immobilization time differed from 5 minutes, up to 60 minutes for DNA. The DNA oxidation currents correlated with time, but started to decrease after 30 minutes, which meant that the selected DNA immobilization time was 30 min. Irreversible anodic peak potential of DHP is determined to be +0.8V. The potency of oxidation for phenolic groups are known to exist, as well as the electrochemical oxidation capacity in hydrazone group of DHP. The electrochemical reactions, hydrazone and phenol groups in particular are highly active for the electrochemical behaviors of DHP. Concentration, pH and immobilization time of DHP were kept optimal as parameters. The investigation of the effect of buffer solution was realized over a broad range of pH values, from acidic to basic. BBS led to the highest oxidation signal of DHP oxidation. 40 $\mu\text{g}/\text{mL}$ of concentration was used throughout the study, showing a better producible and more satisfactory signal. Immobilization time was changed from 10 minutes to 90 minutes for DHP. The increasing of signal was observed by time, which remained almost constant after 45 minutes. 45 min was picked as DHP immobilization time.

Developed method was validated according to parameters of LOD, LOQ, linearity, accuracy and precision. Linearity was observed between 10 to 100 µg/mL concentration. The LOD and LOQ values were calculated to be 3 and 10 µg/mL, respectively.

Calibration curves ($y=mx+n$) were constructed using plots of the peak currents (y) of DHP versus the concentrations (x) of the calibration standards.

Accuracy of method were investigated with intra- and inter-day analyses. For each analyte, three different concentrations were analyzed for intra- and inter-day analyses. Precision of method was obtained from the relative standard deviation (RSD%). The intra- and inter-day precision values were 1.85 and 3.64 µg/mL, respectively. To be more specific, when studying reaction mechanisms on the electrode surface and kinetics parameters as well as oxidation and reduction properties, important and valuable information can be obtained. Thanks to our experiments, scan rates and peak current/potential relationships as well as the kinetic data have been determined. CV is utilized for the determination of the electrochemical data, scan rates and the effect of pH for 40 µg/mL DHP. The shape of the voltammogram is heavily affected by pH of the supporting electrolyte, providing valuable data with regard to the process of electrode that electrons and protons participate in. Hence, the investigation of the effect of pH on the candidate drug is of utmost importance. The highest peak current was acquired by PBS, which is chosen for pH measurements.

CV is also utilized for scan rate study, which helps to determine the diffusion or adsorption controlled process. Physical adsorption of DHP onto the untreated electrode surface was determined by the increased current with scan rate. The potentials of the peaks are also shifted to larger voltage values from +0.3V to +0.6V. 100mV/s scan rate was chosen in order to determine the DHP, for sharp and well-defined signals. Presence of DNA might change the current and peak potential of drug molecule in case of interaction with the compound. Irreversible nature of electron transfer process is verified by positive shift in peak potentials.

To investigate the interaction between guanine and DHP signal, DHP-DNA effect experiments have been conducted. In DPV measurements, 40 µg/mL DHP immobilized PGEs were dipped into 100 µg/mL DNA solution. DHP and DNA were interacted for 5-45 min. The interaction time was chosen as 15 min because the highest oxidation signal differences were obtained between after and before interaction durations.

DHP and guanine oxidation signals were measured in after and before interaction. A decrease has been

noted in guanine current signals following DNA-DHP interaction. This decrease is due to the binding of DHP on DNA, which leads to a compact DNA structure. Hence, oxidation after the interaction becomes more difficult, therefore the guanine oxidation peak currents decrease.

The decrease might be rationalized as a probable harm or defense/security of the oxidizable groups of guanine base in the interim of a candidate molecule interaction with DNA on PGE surface. To detect DNA sites and rational formation/construction of new DNA-targeted molecules, a-such experiments play a vital role. Histogram of oxidation currents of DNA and DHP interaction are presented in **Figure 6**. In addition, the oxidation signals of DHP decreased after its interaction with DNA. In literature, there are many studies which guanine oxidation signal decreases after drug and DNA interaction. However, the decrease or increase redox signals of drug molecules are infrequent (31,32).

The interaction with DHP decreased the current signals of guanine dramatically. The decrease in the DNA oxidation peak currents could be explained as a consequence of the binding of DHP to DNA. The possible reason could be DHP and DNA interaction causes more complex DNA structure and therefore causing oxidization to be more difficult and resulting in a decrease of peak currents for guanine oxidation. The oxidation signal of DHP decreased significantly after the interaction with DNA that confirmed DHP-DNA interaction, leading to DNA structural changes.

In literature, there are studies relevant to DNA-drug interactions of pyridine derivatives analyzed by electrochemical methods. Topkaya et al. (30) investigated DNA and drug interaction of 4-Pyri molecule. They observed that after the interaction with drug molecule, the intrinsic oxidation currents of drug molecule increased while DNA's oxidation currents decreased. In another study, the interaction between pyridine derivate molecule and DNA was analyzed electrochemically. According to the results, it was observed that the oxidation signal of the pyridine derivative increased after its interaction with DNA, while the oxidation signal of guanine decreased (31). In our study, however, oxidation signals of both DNA and candidate drug molecule decreased after DNA and drug interaction. Marin et al. (33) and Teijeiro et al. (34) analyzed the interactions of Mitomycin C and Anthramycin with DNA. They obtained that oxidation signals of DNA and drug molecules decreased after interaction. We obtained similar results in our study showing that DNA and drug molecule's oxidation signals decrease. Wang et al. (35) investigated Promethazine and DNA interactions and they showed that the oxidation signal of Promethazine after its interaction with DNA increased, while the oxidation currents of guanine decreased.

The path for most possible reaction of DHP molecule to occur with OH radicals was analyzed. Gaussian 09 software was utilized for the calculation of optimized geometry and the calculation results were visualized via GaussView 5 software. Subsequently, the determination of the lowest energy states was also conducted by optimization of geometric parameters via Gaussian 09 software. DFT method is employed for the determination of the intermediates for mechanism of photocatalytic degradation relating to DHP, along with the optimization of the structure. Activation energy of the most possible path of reaction was calculated, and their thermodynamically most stable state was determined in gas phase.

CONCLUSION

The electrochemical properties of DHP and interaction between DNA+ DHP were studied for the first time. The interaction between DNA and DHP was measured by DPV. We observed changes in the oxidation signal of DHP and guanine bases of DNA after interaction. The investigations of drug-DNA interaction may provide new compounds to be analyzed for a possible effect on a biomolecular target. In addition, our study enabled a sensitive, fast and easy detection process for interaction between DHP and DNA. The prediction of DHP degradation occurred through intramolecular F1, F2, F3 and F4 ring cleavages, which in turn followed by subsequent •OH radical reactions. The fragments transform into smaller species by this reaction, such as CO₂, NO₃⁻ and NH₄⁺.

ETHICAL DECLARATIONS

Ethics Committee Approval: The ethics committee approval isn't required in the article.

Referee Evaluation Process: Externally peer-reviewed.

Conflict of Interest Statement: The authors have no conflicts of interest to declare.

Financial Disclosure: The authors acknowledge financial support from Tekirdağ Namik Kemal University (Project No: NKUBAP.00.GA.19.217)

Author Contributions: All of the authors declare that they have all participated in the design, execution, and analysis of the paper, and that they have approved the final version.

REFERENCES

- Diculescu VC, Oliveria-Brett AM. In situ electrochemical evaluation of DNA in- teraction with the anticancer drug danusertib nitrenium radical product using the DNA-electrochemical biosensor. *Bioelectrochemistry* 2016; 107: 50-7.
- Wang J. Electrochemical biosensors: Towards point-of-care cancer diagnostics. *Biosensors and Bioelectronics* 2006; 21 :1887-92.
- Palecek E. Oscillographic polarography of highly polymerized deoxyribonucleic acid. *Nature* 1960; 188: 656-7.
- Erdem A, Ozsoz M. Electrochemical DNA biosensors based on DNA-drug interactions. *Electroanalysis* 2002; 14: 965-74.
- Rauf S, Gooding JJ, Akhtar K, et al. Electrochemical approach of anticancer drugs-DNA interaction. *J Pharm Biomed Anal* 2005; 37: 205-17.
- Egli M, Flavell A, Pyle AM, et al. *Nucleic acids in chemistry and biology*. 3th ed. Cambridge- UK: The Royal Society of Chemistry; 2006.
- Yang M, McGovern ME, Thompson M. Genosensor technology and the detection of interfacial nucleic acid chemistry. *Anal Chim Acta* 1997; 346: 259-75.
- Morales KD, Alarcon-Angeles G, Merkoci A. Nanomaterial-based sensors for the study of DNA interaction with drugs. *Electroanalysis* 2019; 31: 1845-67.
- Zheng Y, Yang C, Pu W, Zhang J. Carbon nanotube-based DNA biosensor for monitoring phenolic pollutants. *Microchim Acta* 2009; 166: 21-6.
- Wang J, Ozsoz M, Cai XH, et al. Interactions of antitumor drug daunomycin with DNA in solution and at the surface. *Bioelectrochem Bioenerg* 1998; 45: 33-40.
- Dogan-Topal B, Ozkan SA. A novel sensitive electrochemical DNA biosensor for assaying of anticancer drug leuprolide and its adsorptive stripping voltammetric determination. *Talanta* 2011; 83: 780-8.
- Prinz M, Parlar S, Bayraktar G, et al. 1,4-Substituted 4-(1H)-pyridylene-hydrazone-type inhibitors of AChE, BuChE, and amyloid-β aggregation crossing the blood-brain barrier. *Euro J Pharm Sci* 2013; 49, 603-13.
- Sameem B, Saeedi M, Mahdavi M, Shafiee A. A review on tacrine-based scaffolds as multi-target drugs (MTDLs) for Alzheimer's disease. *Euro J Med Chem* 2017; 128: 332-45
- Jalili-Baleh L, Nadri H, Moradi A, et al. New racemic annulated pyrazolo[1,2-b]phthalazines as tacrine-like AChE inhibitors with potential use in Alzheimer's disease. *Eur J Med Chem* 2017; 139: 280-9.
- Reddy MVK, Rao KY, Anusha G, et al. In-vitro evaluation of antioxidant and anticholinesterase activities of novel pyridine, quinoxaline and s-triazine derivatives. *Environ Res* 2021; 199: 111320.
- Bodor N, Buchwald P. Barriers to remember: brain-targeting chemical delivery systems and Alzheimer's disease. *Drug Discov Today* 2002; 7: 766-74.
- Alptuzun V, Parlar S, Tasli H, Erciyas E. Synthesis and antimicrobial activity of some pyridinium salts.molecules. 2009; 14: 5203-15.
- Chang Y, Jin L, Duan JJ, Zhang Q, Wang J, Lu Y. New conjugated poly(pyridinium salt) derivative: AIE characteristics, the interaction with DNA and selective fluorescence enhancement induced by DNA. *RSC Advances* 2015; 125: 103358-64.
- Xie BP, Qiu GH, Hu PP, et al. Simultaneous detection of Dengue and Zika virus RNA sequences with a three-dimensional Cu-based zwitterionic metal-organic framework, comparison of single and synchronous fluorescence analysis. *Sensors and Actuators B: Chemical* 2018; 254: 1133-40.
- Sun JF, Lu Y, Wang L, et al. Fluorescence turn-on detection of DNA based on the aggregation-induced emission of conjugated poly(pyridinium salt)s. *Polymer Chem* 2013; 14: 4045-51.
- Çintaş ML, Azzouz R, Peauger L, et al. Access to highly enantioenriched donepezil-like 1,4- dihydropyridines as promising anti-Alzheimer prodrug candidates via enantioselective Tsuji allylation and organocatalytic aza-ene-type domino reactions. *J Org Chem* 2018; 83: 10231-40.
- Babu MN, Elumalai K, Srinivasan S, et al. Synthesis and anticholinesterase activity of a novel series of acetazolamide condensed 1,4-dihydropyridines. *Carbon Resour Convers.* 2019; 2: 191-7.

23. Hatipoglu A, Vione D, Yalcin Y, Minero C, Cinar Z. Photo-oxidative degradation of toluene in aqueous media by hydroxyl radicals. *J Photochem Photobiol A: Chem* 2010; 215: 59-68.
24. Atkins PW. *Physical Chemistry*. 6th ed. New York: Oxford University Press; 1998.
25. Mierzejewska KK, Trylska J, Sadlej J. Quantum mechanical studies of lincosamides. *J Mol Model* 2012; 18: 2727-40.
26. Gaussian 09. Revision B.04. Gaussian, Inc. Pittsburgh-PA; 2009.
27. Little TA. Method validation essentials, limit of blank, limit of detection, and limit of quantitation. *Biopharm Int* 2015; 28: 48-51.
28. Palecek E. Adsorptive transfer stripping voltammetry: effect of electrode potential on the structure of DNA adsorbed at the mercury surface. *Bioelectrochem Bioenerg* 1992; 28: 71-83.
29. Kilic T, Topkaya SN, Ozkan Ariksoysal D, et al. Electrochemical based detection of microRNA, mir21 in breast cancer cells. *Biosensors and Bioelectron* 2012; 1: 195-201.
30. Topkaya SN, Karasakal A, Cetin AE, Parlar S, Alptuzun V. Electrochemical characteristics of a novel pyridinium salt as a candidate drug molecule and its interaction with DNA. *Electroanalysis* 2020; 32: 1780-87.
31. Karasakal A, Parlar S, Alptuzun V, Cetin AE, Topkaya SN. A novel molecule: 1-(2,6 dichlorobenzyl)-4-(2-(2-4-hydroxybenzylidene)hydrazinyl) pyridinium chloride and its interaction with DNA. *Electroanalysis* 2021; 33: 1819-25.
32. Aftab S, Kurbanoglu S, Ozcelikay G, et al. Carbon quantum dots co-catalyzed with multiwalled carbon nanotubes and silver nanoparticles modified nanosensor for the electrochemical assay of anti-HIV drug Rilpivirine. *Sensor Actuat B-Chem* 2019; 285: 571-83.
33. Marin D, Perez P, Teijeiro C, Palecek E. Voltammetric determination of mitomycin C in the presence of other anti-cancer drugs and in urine. *Analytica Chimica Acta* 1998; 358: 45-50.
34. Teijeiro C, Red E, Marin D. Electrochemical analysis of anthramycin: hydrolysis, DNA-interactions and quantitative determination. *Electroanalysis* 2000; 12: 963-8.
35. Wang J, Rivas G, Cai X, et al. Accumulation and trace measurements of phenothiazine drugs at DNA-modified electrodes. *Anal Chim Acta* 1996; 332: 139-44.